Signatures of the Rise of Cycle 23

W. A. Dziembowski [1,2], P. R. Goode[2], A. G. Kosovichev[3] and J. Schou[3]

[1] *Warsaw University Observatory and Copernicus Astronomical Center, Poland*

[2] *Big Bear Solar Observatory, New Jersey Institute of Technology, U.S.A*

[3] *W.W.Hansen Experimental Physics Laboratory, Stanford University, U.S.A.*

ABSTRACT

During the rise of cycle 23, we have found a sizeable, systematic evolution of solar oscillation frequencies implying significant changes in the spherically symmetric structure of the sun's outer layers, as well as in its asphericity through a P_{18} Legendre distortion.

We conducted a search for corresponding asymmetries in Ca II K data from Big Bear Solar Observatory (BBSO). We found tight temporal and angular correlations of the respective asphericities up through P_{10}. This result emphasizes the direct role of the magnetic field in producing the frequency changes.

We carried out inversions of the frequency differences and the splitting coefficients assuming that the source of the evolving changes is a varying stochastic magnetic field. With respect to the most recent activity minimum, we detected a significant perturbation in the spherical part at a depth of 25-100 Mm which may be interpreted as being due to a magnetic perturbation, $< B^2 >$, of about $(60KG)^2$ and/or a relative temperature perturbation of about 1.2×10^{-4}. Larger, though less statistically significant perturbations of the interior structure were found in the aspherical distortion.

Subject headings: Sun: interior — Sun: oscillations

1. Introduction

Helioseismic frequencies provide the most accurate global measures of cycle dependent changes in the sun. The advantages of a seismic investigation of the sun are not only the prospect of seeing changes beneath the surface, but also deriving from the frequencies the surfaced averaged parameters which quantify the sun. The real challenge is to connect these global, seismic measures to observed characteristics of the dynamic sun.

Deriving surface averaged quantities (i.e. the P_0-component) from disk averaged observations is a notoriously difficult matter. Here, we faced the problem of absolute calibration using BBSO Ca II K data from full-disk observations. Making such a connection is critical to linking the sun to other stars. Helioseismic measures are especially important here because they provide a unique opportunity to precisely measure surface averages (instead of disk averages).

The observed frequency changes of the solar oscillation multiplets are divided into centroid changes which reflect angular averages over the whole sun, and the changes that are within the individual multiplets. The changes which are not symmetric about the multiplet centroid (the so-called "even-a coefficients") show a strong cycle dependence. The direct source of the cycle dependent changes has been a matter of controversy. However, the only well-established changes are dominated by effects arising in the outermost layers of the sun.

We note that the symmetric part of the multiplet (about the centroid) arises from the sun's differential rotation. Many authors have noted that any cycle-dependent change in this part of the fine structure is insignificant compared with that in the non-symmetric part.

Here, we focus on the part of the spectrum of the oscillation multiplets that shows appreciable cycle dependence.

The sources of the changes are considered to be some combination of variations in temperature, magnetic field and changes in the random velocity field. Goldreich, et al. (1991) proposed that changes in the superficial, random magnetic field is the primary cause of the centroid frequency shifts. This idea has has been criticized by Kuhn (1998) who points out that Goldreich, et al. require a mean, quadratic, near-surface magnetic perturbation, $< B^2 >$ of around $(250G)^2$, while the observations of Lin (1995) and Lin & Rimmele (1999) show a mean, surface field which is significantly weaker. Instead, Kuhn sees a critical role for the variations of the turbulent pressure through the solar cycle. He proposes that changes in the aspherical component of the stresses are responsible for the varying even-a coefficients. This is plausible. However, there is strong evidence that both the centroid and even-a frequency changes closely reflect changes in the magnetic field. In particular, we shall demonstrate here that the evolving asphericities in the even-$a's$ are closely mimicked by the corresponding ones found in the BBSO Ca II K data. One possible way of evading the apparent contradiction Kuhn raises would be to contemplate a significant inward increase in the field intensity. We emphasize that in discussing the field, one has to be careful to distinguish between the direct mechanical effect of the Lorentz force, and the thermal effect arising from the annihilation of the field (referred to as the β-effect) and force's influence on the thermal structure through the perturbation of the convective transport (referred to as the α-effect).

Clearly, we are lacking a basic understanding as to how the frequency changes arise. We need more observational information. The most crucial time period for which we need data is during the rise of the cycle from minimum. Fortunately, we have SOHO data covering that period for the current rising cycle. What we look for in these new data is higher order asymmetries which we correlate with magnetic information from various sources. Further, we look inside the varying sun by inverting the frequency changes and the splitting coefficients.

2. Frequency Changes from SOHO/MDI Data

The data treated here consist of twelve 72-day sets. The first eleven are consecutive and cover the period beginning 1996 May 1 ending 1998 May 31. The last set (which is the first after SOHO operation was recovered) covers 1999 Feb. 3 - 1999 April 15. Each of the data points contains a centroid frequency, $\bar{\nu}_{\ell,n}$, and 36 splitting coefficients, a_k. Each set contains between 1620 and 1680 p-mode multiplets (or ℓ-values from 1 up to 200) and between 120 and 143 p-mode multiplets (of ℓ-values from 123 up to 300).

For each p-mode multiplet, the splittings are defined by

$$\nu_{\ell,n,m} - \bar{\nu}_{\ell,n} = \sum_{k=1} a_k \mathcal{P}_k^{\ell}(m), \tag{1}$$

where $\mathcal{P}$ are orthogonal polynomials (see Ritzwoller & Lavely 1991 and Schou et al. 1994). The remaining symbols in eqn. (1) have their usual meanings. This representation ensures that the $\bar{\nu}_{\ell,n}$ are a probe of the spherical structure while the a_{2k} – the even-a coefficients – are a probe of the symmetrical (about the equator) part of distortion described by the corresponding $P_{2k}(\cos\theta)$ Legendre polynomials. We have

$$\int_0^{2\pi}\int_{-1}^{1}|Y_\ell^m|^2 P_{2k} d(\cos\theta)d\phi = C_{k,\ell}\mathcal{P}_{2k}^{\ell}(m), \quad (2)$$

where

$$C_{k,\ell} = (-1)^k \frac{(2k-1)!!}{k!}\frac{(2\ell+1)!!}{(2\ell+2k+1)!!}\frac{(\ell-1)!}{(\ell-k)!}. \quad (3)$$

We separate the analyses of p and f modes because they have different properties in the outer layers. Our inferences from the f modes only concern possible variations in the seismic solar radius – see §5. For the other remaining sections of the paper, we only consider the centroid frequency of each p-mode and its attendant even-a coefficients.

The even-order splitting coefficients in each of the twelve data sets were fit to the following formula (Dziembowski & Goode, 1991)

$$a_{2k,\ell,n} = a_{2k,\ell,n;\mathrm{rot}} + C_{k,\ell}\frac{\gamma_k}{I_{\ell,n}}, \quad (4)$$

where $a_{2k,\ell,n;\mathrm{rot}}$ represents the effect of centrifugal distortion, which we calculate following the treatment of Dziembowski & Goode (1992); $I_{\ell,n}$ is a measure of the modal inertia (also called the mode mass), and γ_k is the asphericity coefficient corresponding to a P_{2k} distortion. Since our plan is to study the temporal variation of the asymmetry, we therefore eliminate the constant distortion of rotation from the γ coefficients in eqn. (4). The modal inertia was evaluated assuming that all modes have the same radial displacement at the base of solar photosphere. Adopting a value of 10^4 for that displacement, we have $I_{20,19} \approx 1$. The inertia decreases with increasing ℓ or n. Eqn. (4) has also been used to represent changes in centroid frequencies. However, in that case we can determine only a relative γ_0. For this, we chose the first of the twelve MDI sets as the reference.

The $I_{\ell,n}^{-1}$ factor accounts for most of the ℓ and frequency dependence in the splitting coefficients. This was result is due to Libbrecht & Woodard (1990). They used it as evidence that the asphericity responsible for the even-a coefficients is localized well above the lower turning point of modes in the sample – that is, close to surface. Dziembowski & Goode (1991) were able to determine a slight, but significant ν dependence of the γ_1 and γ_2 coefficients from the same data. First, we present the results of fitting constant $\gamma's$ to each of the twelve sets of the even-a coefficients from the SOHO/MDI instrument.

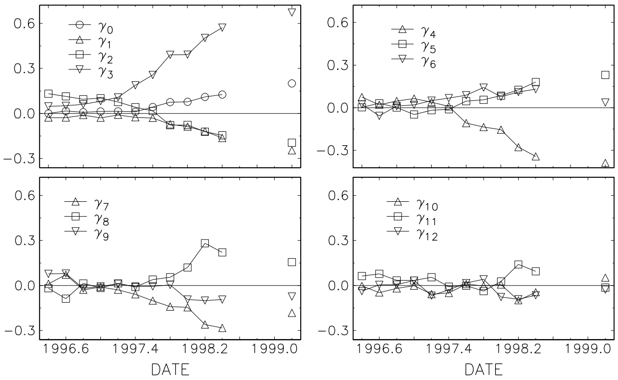

Fig. 1.— Mean asphericity coefficients, γ, (in μHz) from the twelve SOHO/MDI 72-day sets. The first eleven were obtained consecutively during the first two years of SOHO observations (1996 May 1 - 1998 May 31). The twelfth covers 1999 Feb. 3 - 1999 April 15.

In Figure 1, we show the first twelve γ coefficients. This figure is a continuation of Figure 1 in Dziembowski, et al. (1998). Here, we have twelve 72-day long sets, while previously we had only five. We now see clear trends in all four γ-coefficients, γ_0, γ_1, γ_2 and γ_3, whereas before there was no clear trend in γ_0. Furthermore, we now see clear trends in γ_4 and γ_5. This is the first time that we see a significant trend in the asphericity beyond P_6. Beyond P_{10}, there is not always a clear trend, although P_{14} and P_{16} are fairly suggestive. We note that the errors are rapidly increasing with order, k. In detail, the error bars through γ_6 are inside the symbol. The errors increase with order, but even for γ_{12} the error bars span only 4×10^{-2} μHz. Even there, the values are marginally significant, although there is not a clear trend for the γ_{12}. Therefore, we focus our analysis on the first few coefficients in the expansion.

Bhatnagar, Jain & Tripathy (1999) analyzed the centroid changes in the GONG frequencies covering the period 1995 August - 1997 August. They found an increasing tendency over a period comparable to that of our results. However, their quantity characterizing

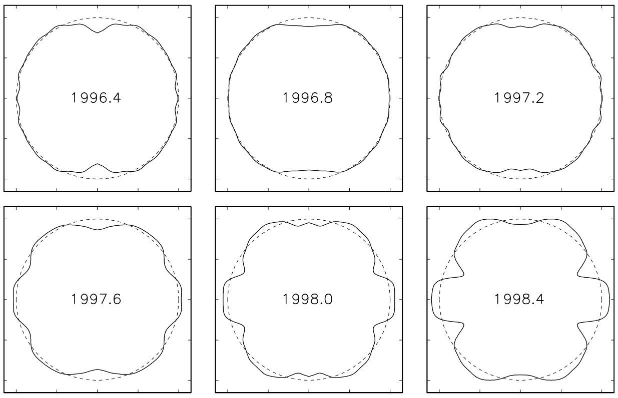

Fig. 2.— Temporal evolution of the solar asphericity over the first two years of MDI data analyzed here. The actual model asphericity is about 300,000 times smaller than shown.

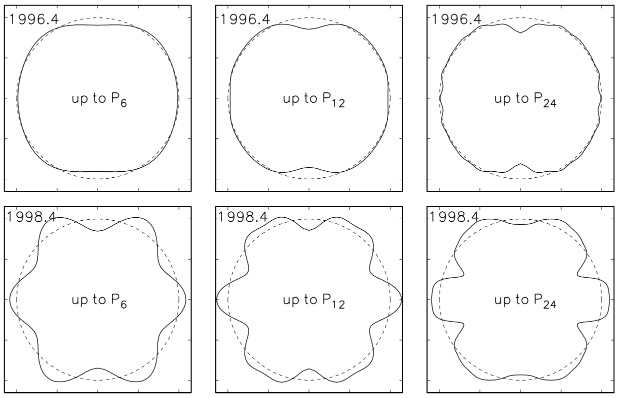

Fig. 3.— The cumulative contribution of the model asphericities over the first two years of MDI data are shown. As in Figure 2, the true model asphericities are amplified about 300,000 times.

the mean frequency change ($\delta\nu$) differs substantially from ours. We find the same mean as they did when we use the MDI data to calculate their quantity. We emphasize however, that the quantity, γ, is the proper characterization of mean frequency changes under the hypothesis that they arise near the surface.

Howe, Komm & Hill (1999) used a lengthier string of GONG frequencies covering the period August 1995 - August 1998. In addition to centroid changes, they analyzed the splitting coefficients up to a_6. They used a weighted average over modes near 3 mHz. We observe a qualitative agreement with their results. However, to compare in detail would require us to do an averaging which we regard as being less informative.

One of our basic problems here is to relate the asymmetries seen in the oscillation frequency multiplets to those in the sun. In Figure 2, we do this with a model and a caricature. The key to the model is noting that one can calculate the rotational distortion of the sun and the corresponding asymmetry that would result in the spectrum of solar oscillations. Of course, centrifugal distortion is dominated by a P_2 shape distortion of the sun which turns out to correspond to a γ_1 of 0.037 μHz. Using this to scale all of the $\gamma's$ from the MDI data and multiplying the resulting distortions by about 300,000, we obtain Figure 2. In Figure 2, we show a caricature of the temporal evolution of the asphericity of the sun implied by the $\gamma's$ of Figure 1. The relative roles of the lower and higher order distortions are illustrated in Figure 3. From this figure, it is clear that a low order expansion gives, at least, a rough picture of the true asymmetry in the oscillation spectrum.

3. Prediction of Low Degree Mode Spectrum for Whole Disk Observations

As described by Dziembowski & Goode (1996), the γ-coefficients from moderate ℓ data can be used to accurately evaluate the frequency changes for low degree modes under the assumption that the cycle dependent perturbation is localized near the surface.

In Figure 4, we plot the frequency dependence of the $\gamma's$ as determined from a three term polynomial fit. For comparison, we show the equivalent curve obtained from BBSO data from 1988 and 1989 . From this, we see that the mid-1998 and early-1999 MDI measures of activity were midway between their counterparts from the last cycle for the years 1988 and 1989 – except for γ_0 which is slightly weaker in 1998 than it was in 1988.

Further, in Figure 5 we show the principle result of this section obtained from the $\gamma's$ of 1998.4. The frequency dependence in $\Delta\nu$ primarily reflects mode inertia. Two points are worth emphasizing. The first is that for full-disk measurements, the anticipated frequency change in these measurements should be weakly ℓ-dependent. This is so because the unresolved peaks in ℓ=2 are dominated by their $m = \pm 2$ components (over m=0) and similarly for ℓ=3 where the mode is dominated by the $m = \pm 3$ components

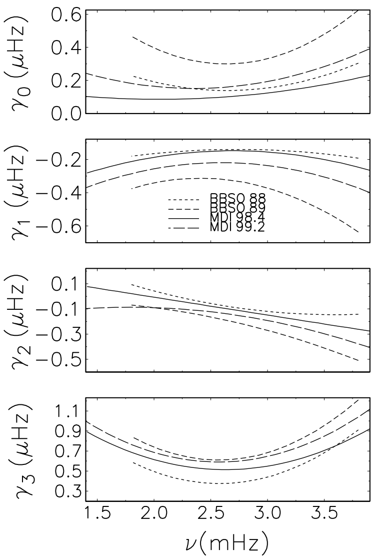

Fig. 4.— $\gamma(\nu)$ dependence of MDI data from the two most recent 72-day sets. Also shown for comparison are the BBSO data from 1988 and 1989.

(over m=1). The second point is that the complete ℓ=2 and 3 multiplets would be visibly asymmetric for high frequencies. As for the scale of the change, the reader should bear in mind that the rotational splitting between adjacent peaks is about 0.45 μHz.

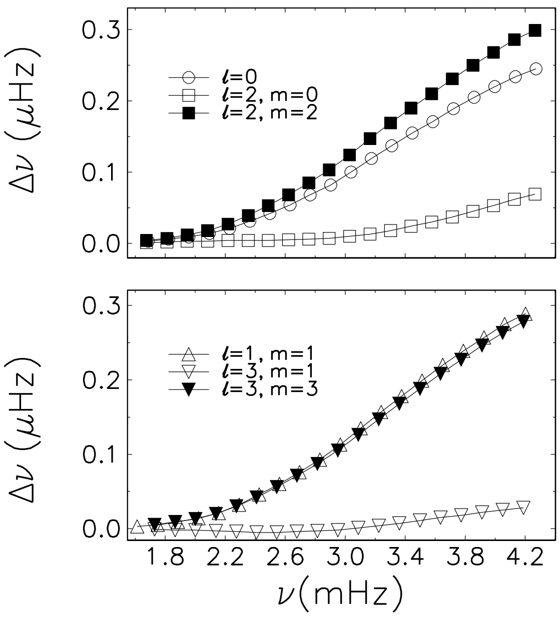

Fig. 5.— The upper panel shows predicted frequency shift, from MDI data, at 1998.4 for ℓ=0 and 2 data as a function of frequency. The same is shown for ℓ=1 and 3 in the lower panel. Note that for each (ℓ, m) mode, the perturbation is the same for m and $-m$.

4. Connection to Other Characteristics of Solar Activity

The close link between the even-a coefficients and the sun's latitudinal thermal structure (Kuhn, Libbrecht, & Dicke 1988) has been demonstrated by Kuhn (1988, 1989); Libbrecht & Woodard (1990) and Woodard & Libbrecht (1991).

Bachmann & Brown(1993) demonstrated a strong correlation among the centroid shifts and various characteristics of activity, including the Mg II 280 nm core-to-wing ratio, the 10.7 cm radio flux, the He I 10830 Åindex, the Kitt Peak magnetic index, the EUV flux, and the Magnetic Plage Index Strength. A similar analysis for the new cycle based on GONG data has been present by Bhatnagar, Jain & Tripathy (1999) in which they find a strong correlation to most of the characteristic indices of activity. They used essentially the same indices as Bachmann & Brown. A similar result was obtained from GONG data by Howe, Komm & Hill, but their results extend over a longer time interval. They also analyzed the behavior of the splitting coefficients (to P_6). Perhaps their most significant find is a clean correlation between the even-a coefficients and the corresponding Legendre coefficients of a fit to the Kitt Peak magnetograms. We report here a similar result based on the BBSO Ca K plage data, but to a higher Legendre order.

First however, we show in Figure 6 the temporal evolution of the $\gamma's$ over thirteen years. This figure is an extension of Figure 4 of Dziembowski, et al. (1998). The extension is the inclusion of seven more 72-day long MDI sets and the inclusion of the corresponding smoothed sunspot numbers. The mean values of the γ coefficients are from various sources including BBSO, LOWL and SOHO/MDI. The BBSO data are from Woodard & Libbrecht (1991), and LOWL data are from Tomczyk (1996). We compare the $\gamma's$ with the monthly averages of smoothed sunspot numbers. Clearly, the BBSO data of 1988 and 1989 give the largest magnitudes of the $\gamma's$, and this corresponds to the first half of the previous sunspot maximum. Unfortunately, we are missing splitting data from the rising phase (1987 or so), as well as from the declining phase of the solar cycle.

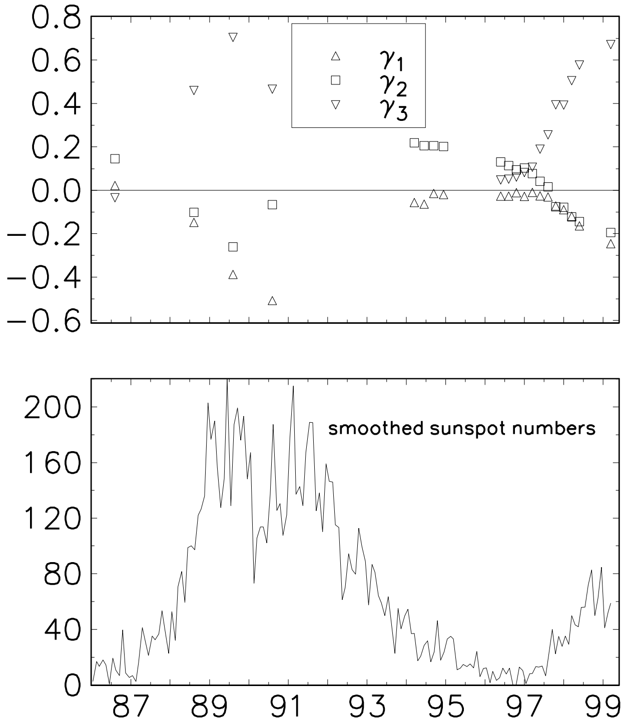

Fig. 6.— Lower panel shows the monthly averages of the sunspot number covering period from 1986 through early 1999. Upper panel shows the mean $\gamma' s$ covering from 1986 through the early 1999. The first cluster of points is from BBSO data (1986-1990). The second is LOWL (1994) and the third is MDI data.

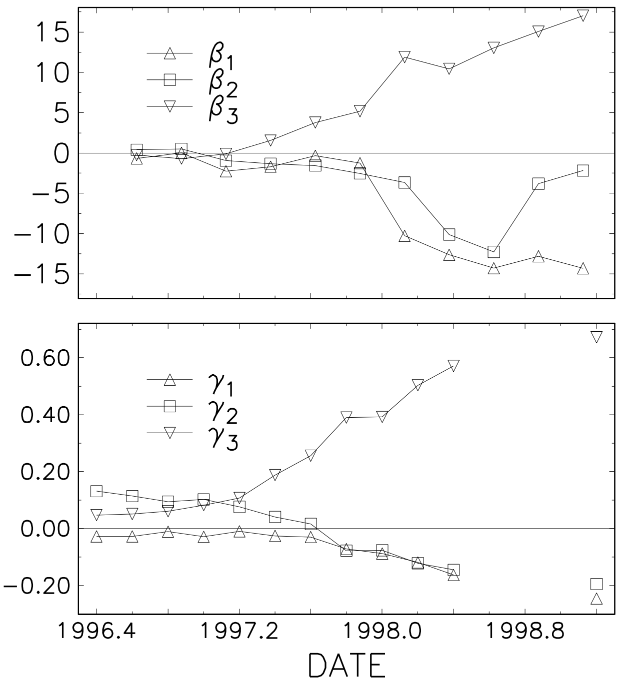

Fig. 7.— Upper panel shows the quarterly P_2, P_4 and P_6 distortions in the BBSO Ca II K data. This is to be compared to the corresponding $\gamma' s$ from the MDI data. The $\beta' s$ are from a Legendre fit and the ordinate is in arbitrary units.

The errors in the BBSO and LOWL $\gamma' s$ are about twice as large as those in SOHO/MDI, but they are still relatively small and would not be visible in Figure 6.

For the current rising cycle, the rapid rise, especially of the of P_6 coincides with the rise of the sunspot number. Based on a comparison with the previous maximum, it can be noted that the maximum value of γ_3 (at 1999.2) corresponds to a much higher activity level than reflected in the sunspot number. The difference can only be partially explained by the difference in mode sets used to infer the γ in the BBSO and MDI sets.

In Figure 7, we show a series of Legendre decompositions of successive quarterly averages of daily BBSO Ca II K images using one image per day. We also show the corresponding $\gamma' s$ from the MDI data. In Figure 7, we show the β_2, β_4, and β_6 coefficients of that decomposition. We do not show the k=0 term because of problems in absolute calibration. In Figure 7, there is a systematic correlation between the $\beta' s$ of the quarterly Ca K data and the corresponding $\gamma' s$. The close agreement between the $\beta' s$ and $\gamma' s$ continues through P_{10}, as can be seen in Figure 8. The breakdown in the agreement comes for γ_6 which lacks the clear trend evident in the lower ranking terms. In addition, there is not a compelling correlation between β_6 and γ_6. Further, the errors are starting to become appreciable by this point. Still, it is impressive that there is such a strong correlation in the temporal evolution, from P_2 through P_{10}, between a measure of the magnetic field and the asymmetries in the oscillation multiplets.

Another thing to notice in Figure 7 is that the P_4 asymmetry (β_2) in the years of solar minimum is much less visible than the corresponding helioseismic asymmetry expressed by γ_2. Is this evidence of a distinct origin of γ_2?

While we see the same trends in the $\beta' s$ and $\gamma' s$ in Figures 7 and 8, we also see some differences. For

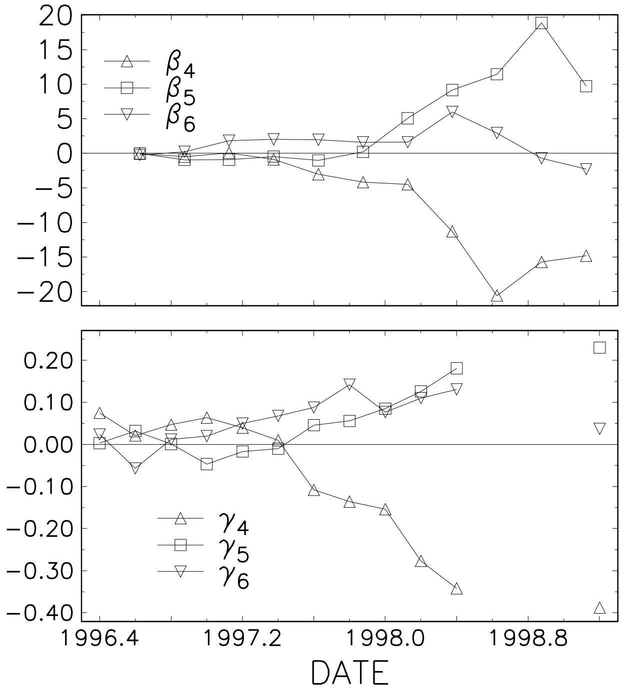

Fig. 8.— Upper panel shows the quarterly P_8, P_{10} and P_{12} distortions in the BBSO Ca II K data (in arbitrary units). This is to be compared to the corresponding $\gamma's$ from the MDI data.

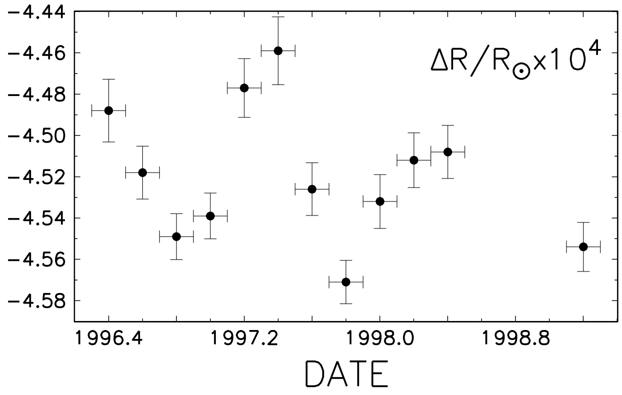

Fig. 9.— Relative differences in the radius of the sun, multiplied by 10^4, inferred from f mode frequencies and the standard solar model (Christensen-Dalsgaard, et al. 1996).

instance, the ratio of γ_3 to γ_1 or γ_2 is about three times the values of their β counterparts. The reversal of the decreasing trend in the β_2 coefficient does not have its counterpart in the behavior of γ_2. However, based on the behavior of γ_2 during the previous cycle (see Figure 6) we may expect that such a reversal should happen soon.

5. Changes in the Solar Radius

Spruit (1998) says that "if variations in $\frac{\Delta R}{R}$ much exceeding a few time 10^{-7} were reliably detected, the implications would be much more serious than a mere contradiction between, say, a dynamo theory and observations of the solar cycle." The changes in the radius inferred from fundamental mode frequencies reported by Dziembowski, et al. (1998) exceed this by one order of magnitude.

In Figure 9, we show the results of radius variations now extended to include the full twelve sets of MDI f-mode data available. Here, the amplitude of the changes is even larger than we reported earlier for the first five datasets. However, there is no visible trend, unless one has a fertile imagination and sees an oscillation. We cannot offer any explanation for the observational results and we warn readers against interpreting the results too literally, because the relation between the true radius and that inferred from f-modes is not clear.

We note that the lack of a trend is in sharp contrast with the behavior of the sun's spherical symmetry as reflected in γ_0 over the same interval shown in Figure 1.

6. Search for an Interior Signature of Solar Cycle Variability

The main advantage of a helioseismic probing of solar variability over the cycle is the prospect of detecting changes beneath the photosphere. There is strong evidence that most of the signal we see in the $\gamma's$ arises close to the surface. Of course, it would be important to know exactly how close, and whether or not we can see a signal from deeper layers.

The problem of localizing the perturbation cannot be completely separated from its physical cause. Goldreich, et al. (1991) derived a formula connecting p-mode frequency changes to changes in entropy and magnetic field intensity. They used their formalism to assess the required field intensity, and infer the localization of the perturbation needed to explain the changes in centroid frequencies. They concluded that the main contribution arises from the photospheric region, while there is significant contribution from much higher layers for high frequency modes. The latter conclusion is based on the observation that there is a sharp drop in $\delta\nu$ at very high frequencies (above 3.5 mHz). We stress that we do not find such an effect in the SOHO data. There is some saturation in the growth of $\delta\nu$ at high frequencies. This is primarily a property of mode inertia. After an initially sharp decrease with ν, the inertia reaches its maximum at about 3.5 mHz and then slowly declines. The intrinsic behavior of the spherically symmetric part of the perturbation is best revealed in γ_0, shown in Figure 4. Here one observes an increase rather than a decrease in γ_0 above 3.0 mHz. The weak dependence of γ_0 on frequency (the same holds for the other $\gamma' s$) points to a localization of the perturbation close to the photosphere where we normalize our eigenfunctions for evaluating mode inertia. Unfortunately, not much more can be inferred from the weak frequency dependence of the $\gamma' s$.

The observational evidence strongly supports the view that, more or less, there is a direct role of the magnetic field in producing the frequency changes. The formalism of Goldreich et al, in principle, describes radial pulsation. However, it may be applied to all modes, if the perturbation is localized well above the modes' lower turning point. This restriction is a clear shortcoming of the formalism when applied near the surface because helioseismic diagnosis rests primarily on differential sampling, which depends mostly on ℓ.

With this in mind, we developed a formulation which is free from the aforementioned shortcomings. In particular, we developed formulae connecting the magnetic field and the resulting perturbation of the thermodynamical quantities, and their combined effect on the oscillation frequencies. Furthermore, we considered the θ dependence of the mean magnetic field which enabled us to develop corresponding connection formulae for the even a-coefficients.

We focus our attention on the case of an isotropic, random field. Specifically, we set

$$\overline{B_j B_k} = \frac{B^2(r,\theta)}{3}, \tag{5}$$

where the quantities in the formula have their usual meanings. Then, we represent B^2 in the form

$$B^2(r,\theta) = 24\pi \sum h_k(r) P_{2k}(\cos\theta). \tag{6}$$

Of course, there may exist an antisymmetric component with respect to the equator, but in a linear treatment of the perturbation of the magnetic field, such effects do not contribute. Mechanical equilibrium implies

$$\frac{d}{dr}(p_k + h_k) = -\rho_k g - \rho \frac{d\phi_k}{dr} \tag{7}$$

and

$$p_k + h_k = -\rho\phi_k \text{ for } 2k > 0, \tag{8}$$

where the subscript k denotes the corresponding coefficient of the expansion of the respective quantities.

Note that eqns. (7) and (8) imply that

$$\phi_k \equiv \rho_k \equiv 0 \tag{9}$$

and

$$\frac{u_k}{u} = \frac{p_k}{p} = -\frac{h_k}{p}, \tag{10}$$

where $u = \frac{P}{\rho}$. Except for the ionization zones, we have $\frac{u_k}{u} \approx \frac{T_k}{T}$.

In the adopted approximation, the magnetic field just acts like an additional pressure. It is well known that as long as such a pressure is isotropic, it does not disrupt the star's spherical symmetry, insofar as the dynamical parameters are concerned.

Eqn. (10) implies that zones with stronger fields should be cooler. Of course, in order to maintain thermal balance, an aspherical component must be present in the convective flows – a close analog to the classical meridional circulation in rigidly rotating stars. Here, we assume that the effects of such flows may be ignored in eqns. (7) and (8).

There are important physical distinctions resulting from the differences between the spherical and non-spherical parts of the perturbation. For the spherical part, the connection between h_k and the corresponding thermodynamical parameters requires that one consider the star's thermal balance. For the non-spherical part, mechanical equilibrium conditions alone suffice. For the inversion formalism, this means that for the radial case we have to consider two unknown structural functions, $\Delta u \equiv u_0$ and $\Delta h \equiv h_0$. The connection formula that we derived is

$$\frac{\Delta\nu}{\nu} = \int_0^1 [\mathcal{K}_{u,0}\frac{\Delta u_0}{u} + \mathcal{K}_{h,0}\frac{\Delta h}{p}] d\tau, \tag{11}$$

where τ is the acoustic radius,

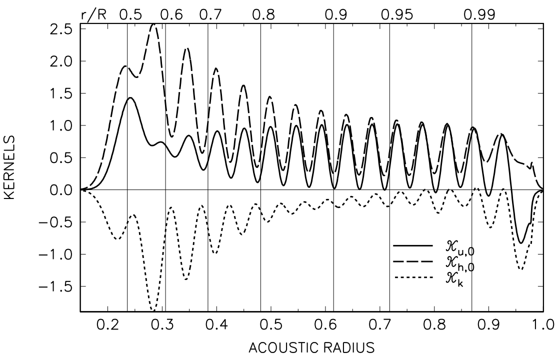

Fig. 10.— Kernels, $K_{u,0}$, $\mathcal{K}_{h,0}$ and $\mathcal{K}_k$ vs. the acoustic radius and fractional radius.

$$\tau = \int_0^r \frac{dr'}{c} [\int_0^R \frac{dr'}{c}]^{-1}.$$

On the other hand, for the splitting coefficients which reflect the non-spherically symmetrical part, we make an approximation. The approximation here is that we ignore one term which can only be appreciable near the lower turning point. This term mixes the h_k term with its counterparts of lower rank. This term arises from the modification of the Lorentz force by the oscillations. In our preliminary analysis here, we use this approximation as well as eqn. (10) to express h_k in terms of u_k. Thus, we obtain

$$a_{2k} \cong C_{k,s} \int \mathcal{K}_{u,k} \frac{u_k}{u} dr. \tag{12}$$

The explicit form and derivation of eqns. (11) and (12) will be published elsewhere, Dziembowski and Goode (in preparation).

A potentially significant contributor to the time dependent perturbation is the Reynold's stresses. We do not consider them here, but plan to address their role in a future work.

Our sole aim here is to search for any signature of changes in the interior.

In Figure 10, we show examples of the three kernels in eqns. (11) and (12) for ℓ=20, ν=3 mHz and n=15. The important thing to notice is that throughout most of the interior, the two kernels, $\mathcal{K}_u$ and $\mathcal{K}_h$, are very similar. This sends a rather grim message about the prospect of disentangling the magnetic field and temperature perturbations.

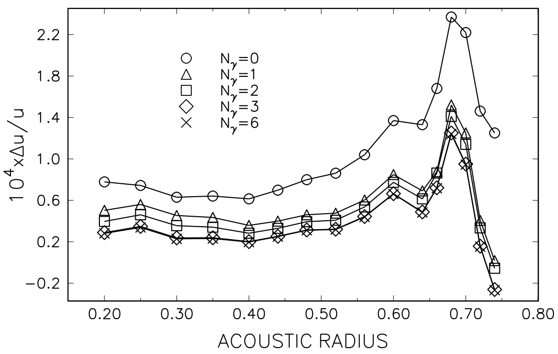

Fig. 11.— Result of inversions of the frequency differences for the relative temperature perturbation between 1999.2 and 1996.4. N_γ denotes number of terms in the polynomial representation of $\gamma_0(\nu)$; N_γ=0 means that effects of the near surface perturbation have not been removed.

6.1. Inversion for Spherically Symmetric Changes

Because of the similarity between the two kernels, $\mathcal{K}_{u,0}$ and $\mathcal{K}_{h,0}$, we did not attempt to solve a simultaneous inversion problem. Rather, we solved separate inverse problems, ignoring respectively the u_0 and then the h_0 contribution. We used an optimal averaging method (SOLA, developed by Pijpers and Thompson 1992).

In Figure 11, we see how various treatments of the near-surface cycle-dependent perturbation effect the inversion for the temperature difference. Removing γ_0/I from the measured $\frac{\Delta\nu}{\nu}$ values amounts to subtracting the unresolved, near surface contribution which apparently makes up most of the $\frac{\Delta\nu}{\nu}'s$. We see that there is a cross-talk problem. However, there is a common feature, and that is the rise of $\frac{\Delta u}{u}$ between 0.5 and 0.7 of the acoustic radius. Furthermore, the differences among the results obtained with various $N_\gamma > 0$ are less than the 1σ errors shown in Figure 12. The γ_0 terms used to obtain the results shown in Figure 12 were obtained with a three term polynomial representation of the $\gamma(\nu)$ dependence, as shown in Figure 4. The fact is, however, that the results are insensitive to the number of terms in the polynomial – a constant γ gives a similar result. What this means to us is that the contribution to $\frac{\Delta\nu}{\nu}$ seen in Figure 11 cannot be eradicated by a judicious adjustment of the near surface contribution.

We believe that removing γ_0 is more realistic than leaving it in. There are many uncertainties in mod-

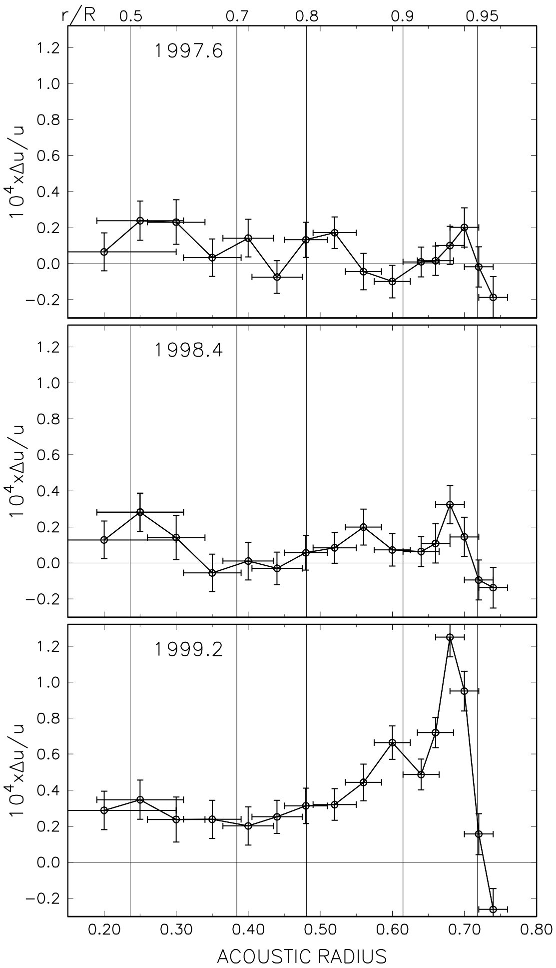

Fig. 12.— Inversions of the frequency differences between indicated years and 1996.4 with the near surface contribution eliminated.

eling the outermost part of the sun (see Kosovichev, 1995, for a recent discussion), and there are various possible sources of frequency changes arising there that are difficult to disentangle. In all subsequent analysis, we remove the near surface effect by subtracting a three term representation of $\gamma(\nu)$. Still, there is a good part of the sun's interior where even with the data we have in hand, one could not build a satisfactory kernel. In the three panels of Figure 12, we show the temporal evolution of the perturbation with respect to 1996.4, the time of activity minimum. The most significant result from all of our inversions is the increase in $\Delta u/u$ between 0.4 and 0.68 (where it peaks) of the acoustic radius, at the peak, we find a value which exceeds the errors by a factor of 10. We

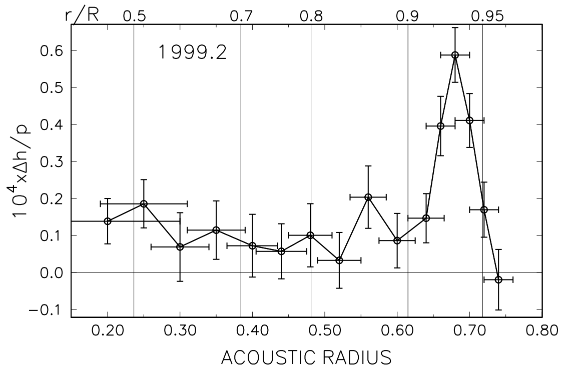

Fig. 13.— Inversion of the frequency differences between 1999.2 and 1996.4 to determine the magnetic field changes with the near surface contribution removed.

also see peaks at the same location in the inversion of earlier data sets, but of much lower amplitude.

If indeed the peak at 0.68 were mostly due to a temperature perturbation, then the $\frac{\Delta u}{u}$ value of $\approx 1.2 \times 10^{-4}$ inferred from the last data sets means a 400°K temperature perturbation at a depth of 45 Mm.

In Figure 13, we show the results of inversions for Δh with Δu set to zero. There are differences in the details as compared with Figure 12, however the peak at 0.68 remains. The value of Δh at the peak ($6{\times}10^{-5}$) implies a $< B^2 >$ of $(60KG)^2$ which is at the lower limit of the current best guess of that quantity at the base of the the convection zone (D'Silva and Choudhury 1993, D'Silva and Howard 1993); however, it is far greater than the current estimates of $< B^2 >$ on the sun's surface – about $(0.07KG)^2$, Kuhn (1998).

Perhaps the peak at 068 is an artifact of the data analysis. However, one argument in its favor comes from the fact that Howe, et al., see the same peak. They inverted the frequency differences using the GONG data. They performed a regularized least-squares inversion which makes it difficult to fully believe the features they calculate. In fact, they did not regard the feature of interest here as being significant. Nonetheless, when we look at their Figure 6, we notice that they also find a peak near the same point that we do.

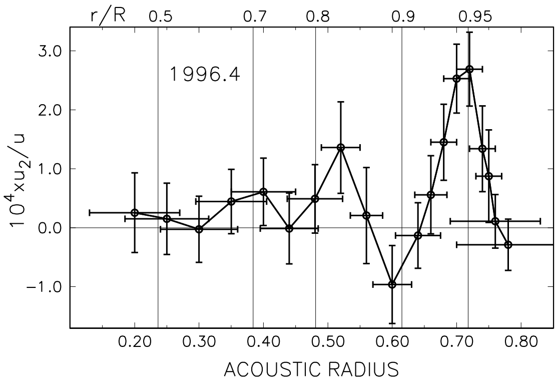

Fig. 14.— Inversion of the a_4 splitting coefficients for the P_4 temperature perturbation at activity minimum.

6.2. Inversion for Angular Structure

We look for the signature of the interior by inverting the a-coefficients for which the signal is the strongest.

As in the inversions for radial structure, we remove the appropriate γ_k coefficient from a_{2k} in eqn. (12). Explicitly, we remove the contribution of the $\frac{C_{k,l}\gamma_k(\nu)}{I_{n,l}}$ to the a_{2k}.

We begin our analysis, with the a_4-coefficients from 1996.4. Throughout the solar minimum, the a_4 coefficients were the only appreciable oscillation coefficients describing solar asymmetry. The result of our inversion for 1996.4 is shown in Figure 14. The feature of interest here is the sharp rise in the relative temperature in the interval between 0.60 and 0.70, which is closer to the surface than the peak in the inversions for radial structure. The result has a 4σ significance. Note that the maximum value of $\frac{u_2}{u}$ is about twice as large as the maximum value of $\frac{\Delta u_0}{u}$ seen in Figure 12. The values of the corresponding $\gamma's$ (see Figure 1) are similar. The positive values of u_2 imply negative values of the magnetic field coefficient of eqn. (6). That is, a higher temperature implies a lower magnetic field.

We remark that inversions of $a_4's$ of subsequent datasets fail to reveal any persistent temporal trend – in contrast to what we have seen in the behavior of γ_2. The only persistent feature is the peak at acoustic radius $\tau \approx 0.72$.

In Figure 15, we show the results of inversions of the a_6 – the dominant terms in the years of higher activity, see Figure 1. We selected three data sets from the phase of high activity.

As in the previous case, the peak is in shallower layers (at 0.76 in acoustic radius or a depth of 24 Mm). The maximum value of $\frac{u_6}{u}$ is even larger than the maximum value of $\frac{u_4}{u}$. The results are marginally significant at a 3σ level. The plots illustrate a lack of any temporal trend. Thus, we attach less weight to them than to the results from the inversions for the radial structure.

We should stress, however, that a sound speed perturbation of a similar size and localization has been seen before. Kosovichev (1996) found it from an inversion of time-distance data taken in 1991 – that is, during the previous solar maximum.

7. Conclusions

We find a rapid rise in the seismic signature of solar activity between 1997.5 and 1998.4 (the end of the MDI dataset). The signatures are the even a coefficients describing asymmetries in oscillation multiplets. For the first time, we were able to determine significant asymmetries extending up to P_{18}. We compared the temporal and angular asymmetries of the sun from oscillations from SOHO/MDI with BBSO Ca II K data. We found clear temporal and angular correlations, through P_{10}, between the two extending over the rising phase to date. The comparison indicates a direct link between changes in the surface magnetic field and solar oscillation frequencies.

We also examined changes in the sun's radial structure implied by the changes in centroid frequencies of oscillation multiplets. The typical frequency change at 3 mHz was about 0.1 μHz over the interval considered.

We used information about the sun's asymmetries and radial structure changes to predict the multiplet structure for low degree modes for spatially unresolved observations. Further, we showed that there should be a significant asymmetry in the full multiplet structure for low ℓ.

We used data on f-modes to infer information about changes in the sun's seismic radius. We found relative changes on the order of 10^{-5}, but without a visible trend.

We searched for a signature of solar cycle changes in the sun's interior by means of optimally averaged inversions of the frequency differences and the splitting coefficients. We believe that we obtained a significant result from the former analysis. We found the

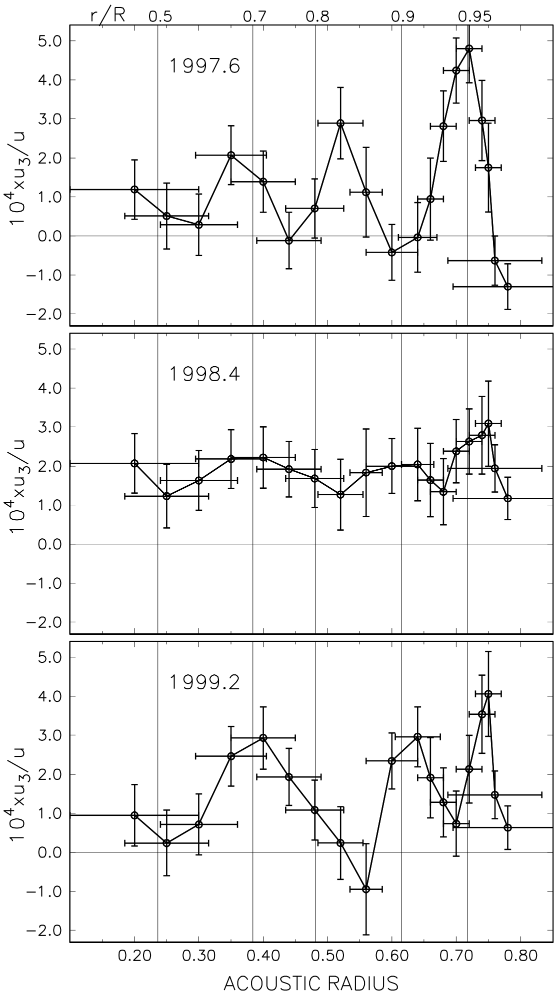

Fig. 15.— Inversion of the a_6 splitting coefficients for the relative P_6 temperature perturbation from three time periods.

most significant change in the layer located at a depth ranging between 25 and 100 Mm with a peak at 45 Mm. The perturbation may be due to a relative temperature increase peaking at 12×10^{-5}, or an increase in $< B^2 >$ peaking at $(60KG)^2$ (or some combination thereof). We are unable to disentangle the two.

We can only speculate about the nature of this perturbation. Since the implied field intensity is significantly stronger than that on the sun's surface, this may perhaps indicate a role of convective downdrafts in preventing the field from reaching the photospheric layers.

The inversion of the splitting coefficients reveals, in principle, the angular structure of the perturbation, yields less significant results. The maximal value of the perturbation occurs in the outermost layers – peaking at a depth of about 30 Mm beneath the surface. Presumably such a field would be dissipated *in situ*.

This is a preliminary work. In the future, we plan several interrelated projects: 1) follow the changes in the $\gamma's$ during the current rising phase of activity and subsequently, through the maximum and declining phase of cycle 23. After all, we lack corresponding information from cycle 22; 2) invert even-$a's$ from data with higher ℓ values to improve the spatial resolution in the outer layers; 3) study intensity bands in various wavelengths to get information on the vertical distribution of the temperature perturbation; 4) develop the connection formulae linking frequency changes to temperature, magnetic fields and velocity fields assuming various models of the random fields; and 5) consider the energy balance in the outer layers taking into account the effects of field dissipation, as well as the modification of the convective transport by the field. This is essential because there is no unique interpretation of the $\delta\nu's$ and the even-$a's$, so that ultimately the interpretation requires physical models which then must be compared with data through a forward problem. Furthermore, this is needed to link luminosity and irradiance variations. The requisite information about the luminosity is in the $\delta\nu's$, but we need models to decode it.

SOHO is a project of international cooperation between ESA and NASA. This research was supported by the SOI-MDI NASA contract NAG5-3077 at Stanford University, and partially supported by NSF-ATM-97-14796 and NASA-NAG5-4919 grants to Big Bear and KBN-2-P03D-014-14 to W.A.D..

REFERENCES

Bachmann, K. T. & Brown, T.M., 1993, ApJ, 411, L45

Bhatnagar, A., Jain, K., & Tripathy, S.C., 1999, in GONG99 Proceedings, in preparation

Christensen-Dalsgaard, J. et al. 1996, Science, 272, 1286

Duvall, T. L., Jr., D'Silva, S., Jefferies, S. M., Harvey, J. W., Schou, J. 1996, Nature, 379 , 235

Dziembowski, W. A. & Goode, P. R. 1991, ApJ, 376, 782

Dziembowski, W. A. & Goode, P. R., 1992, ApJ, 394, 670

Dziembowski, W. A. & Goode, P. R., 1996, A&A, 317, 919

Dziembowski, W. A.& Goode, P. R., DiMauro, M.P., Kosovichev, A.G., Schou, J., 1998, ApJ, 509, L456

Dziembowski, W. A.& Goode, P. R., Schou, J., Tomczyk, S. 1997, A&A, 323, 231

Goldreich, P. Murray,N.,Willette,G., & Kumar, P.,1991, ApJ, 370, 752

Howe, R., Komm,R., & Hill, F., 1999, ApJ, submitted.

Kosovichev, A. G. 1995, in Proc. 4th SOHO Workshop, ESA SP-376, ESTEC, Noordwijk, p. 1.

Kosovichev, A. G. 1996, ApJ, 461, L55

Kosovichev, A. G. et al. 1998, in Proc. IAU Symp. 185, New Eyes to See Inside the Sun and Stars, F.-L.Deubner et al. (eds), 157

Kuhn, J. R., 1988, ApJ, 331, L131

Kuhn, J. R., 1998, in Structure and Dynamics of the Interior of the Sun and Sun-like Stars, Eds. S. Korzennik & A. Wilson, ESA, 871

Kuhn, J. R., Bush, R.I., Scheick, X., & Scherrer, P.H. 1998, Nature, 392, 155

Kuhn, J. R., Libbrecht, K. G., & Dicke, R. H. 1996, Science, 242, 908

Kuhn, J. R. & Stein, R., 1996, ApJ, 463, L119

Libbrecht, K. G., 1988, ApJ, 334, 510

Libbrecht, K. G.& Woodard, M. F., 1990, Nature, 345, 779

Lin, H., 1995, ApJ, 446,421

Lin, H. & Rimmele, R.R., 1999, ApJ, 514, L448

Pijpers, F. P. & Thompson, M.J., 1995, ApJ, 488, L57

Ritzwoller, M. H. & Lavely, E. M., 1991, ApJ, 369, 557

Schou, J., Christensen-Dalsgaard, J. & Thompson, M. J., 1994, ApJ, 433, 289

Schou, J., Kosovichev, A. G., Goode, P. R., & Dziembowski, W. A., 1997, ApJ, 489, L197

Spruit, H. , 1998, in International Astronomical Union. Symposium no. 185. New Eyes to See Inside the Sun and Stars, edited by Franz-Ludwig Deubner, Joergen Christensen-Dalsgaard, and Don Kurtz. Kyoto, Japan, 18-22 August, 1997, p.103.

Tomczyk, S., 1996, private communication

Woodard, M. F. & Libbrecht, K. G., 1991, ApJ, 374, L61

Woodard, M. F. & Libbrecht, K.G. 1993, ApJ, 402, L77

This 2-column preprint was prepared with the AAS LATEX macros v4.0.